Semi-automatic Brain Lesion Segmentation in Gamma Knife Treatments Using an Unsupervised Fuzzy C-Means Clustering Technique

Leonardo Rundo, Carmelo Militello, Salvatore Vitabile, Giorgio Russo, Pietro Pisciotta, Francesco Marletta, Massimo Ippolito, Corrado D'Arrigo, Massimo Midiri and Maria Carla Gilardi

Abstract MR Imaging is being increasingly used in radiation treatment planning as well as for staging and assessing tumor response. Leksell Gamma Knife® is a device for stereotactic neuro-radiosurgery to deal with inaccessible or insufficiently treated lesions with traditional surgery or radiotherapy. The target to be treated with radiation beams is currently contoured through slice-by-slice manual segmentation on MR images. This procedure is time consuming and operator-dependent. Segmentation result repeatability may be ensured only by using automatic/semi-automatic methods with the clinicians supporting the planning phase. In this paper a semi-automatic segmentation method, based on an unsupervised Fuzzy C-Means clustering technique, is proposed. The presented approach allows for the target segmentation and its volume calculation. Segmentation tests on 5 MRI series were performed, using both area-based and distance-based metrics. The following average values have been obtained: $DS = 95.10$, $JC = 90.82$, $TPF = 95.86$, $FNF = 2.18$, $MAD = 0.302$, $MAXD = 1.260$, $H = 1.636$.

Keywords Semi-automatic segmentation · Gamma knife treatments · Unsupervised FCM clustering · MR imaging · Brain lesions

L. Rundo · C. Militello (✉) · G. Russo · P. Pisciotta · M.C. Gilardi
Istituto di Bioimmagini e Fisiologia Molecolare - Consiglio Nazionale delle Ricerche (IBFM-CNR), Cefalù (PA), Italy
e-mail: carmelo.militello@ibfm.cnr.it

S. Vitabile · M. Midiri
Dipartimento di Biopatologia e Biotecnologie Mediche (DIBIMED), Università degli Studi di Palermo, Palermo, Italy

F. Marletta · M. Ippolito · C. D'Arrigo
Azienda Ospedaliera Cannizzaro, Catania, Italy

S. Bassis et al. (eds.), *Advances in Neural Networks*, Smart Innovation, Systems and Technologies 54, DOI 10.1007/978-3-319-33747-0_2

1 Introduction

Magnetic Resonance Imaging (MRI) of the brain can provide images of very high quality revealing detailed information especially concerning the extent of abnormalities, and thus has a great potential in radiotherapy planning of brain tumors [1]. Currently, MRI is considered to be superior to Computed Tomography (CT) in determining the extent of tumor infiltration [2]. Leksell Gamma Knife® (Elekta, Stockholm, Sweden) is a device for stereotactic neuro-radiosurgery to deal with inaccessible or insufficiently treated lesions with traditional surgery or radiotherapy [3, 4]. Gamma Knife (GK) surgery does not require the skull to be opened for treatment. The patient is treated in one session and normally can go home the same day. Radioactive beams (generated by cobalt-60 sources) are focused on the target through a metal helmet (Fig. 1a). Before treatment, a neurosurgeon places a stereotactic head frame on the patient, used to accurately locate the target areas and to prevent head movement during imaging and treatment. After treatment planning phases, the actual treatment begins and the head frame is attached to the Gamma Knife metal helmet (Fig. 1b).

Nowadays, the target volume (Region Of Interest, ROI) is identified with slice-by-slice manual segmentation on MR images only, acquired while the patient is already wearing the stereotactic head frame just before treatment. This procedure is time consuming, because many slices have to be manually segmented in a short time. Manual segmentation is also an operator-dependent procedure.

The repeatability of the tumor boundaries delineation may be ensured only by using automatic/semi-automatic methods, supporting the clinicians in the planning phase [5–7]. Consequently, this improves the assessment of the Gamma Knife treatment response. As illustrated in [2], semi-automated approaches provide more reproducible measurements compared to conventional manual tracing. This was proved by quantitatively comparing intra- and inter-operator reliability of the two methods.

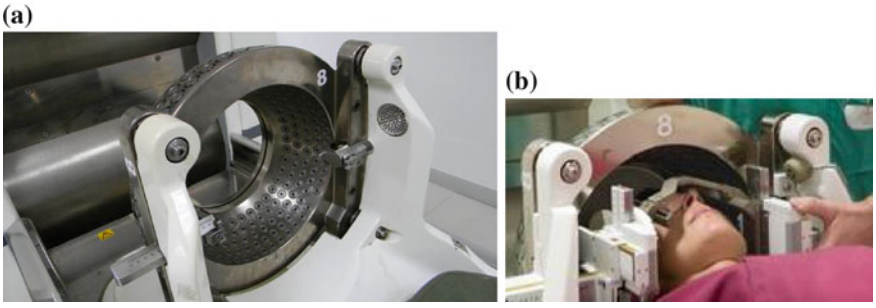

Fig. 1 Leksell Gamma Knife® equipment: **a** metal helmet with collimators; **b** metal helmet with patient positioned, while wearing the stereotactic head frame

In this paper a semi-automatic segmentation method, based on the unsupervised *Fuzzy C-Means (FCM)* clustering technique, is proposed. This approach helps segment the target and automatically calculate the lesion volume to be treated with the Gamma Knife® device. To evaluate the effectiveness of the proposed approach, initial segmentation tests, using both area-based and distance-based metrics, were performed on 5 MRI series.

This manuscript is organized as follows: Sect. 2 introduces an overview of brain lesion segmentation from MR images; Sect. 3 describes the proposed segmentation method; Sect. 4 illustrates the experimental results obtained in the segmentation tests; finally, some discussions and conclusions are provided in Sect. 5.

2 Background

In the current literature there are no works closely related to the segmentation of target volumes for Gamma Knife treatment support. We focused on papers dealing with target segmentation in radiotherapy.

The authors of [8] argue that it is better to use local image statistics instead of a global ones. A localized region-based *Active Contour* semi-automatic segmentation method (by means of *Level Set functions*) was applied on brain MR images of patients to obtain clinical target volumes. A similar method is reported in [9], in which *Hybrid Level Sets (HLS)* are exploited. The segmentation is simultaneously driven by region and boundary information.

In this context, Computational Intelligence techniques are often exploited. Mazzara et al. [10] present and evaluate two fully automated brain MRI tumor segmentation approaches: supervised *k-Nearest Neighbors (kNN)* and automatic *Knowledge-Guided (KG)*. Analogously, an approach based on *Support Vector Machine (SVM)* discriminative classification is proposed in [11]. For these supervised methods, however, a training step is always required. Lastly, Hall et al. [12] extensively compared literal and approximate *Fuzzy C-Means* unsupervised clustering algorithms, and a supervised *computational Neural Network*, in brain MRI segmentation. The comparison study suggested comparable experimental results between supervised and unsupervised learning.

3 The Proposed Segmentation Approach

In this section, a semi-automatic segmentation approach of the brain lesions from axial slices of brain MRI concerning Gamma Knife patients is presented. The proposed method combines existing literature methods in a smart and innovative fashion, resulting in an advanced clustering application for brain lesion segmentation. The user selects only a bounding area containing the tumor zone and no parameter setup is required (Fig. 2). Thereby, operator-dependence is minimized.

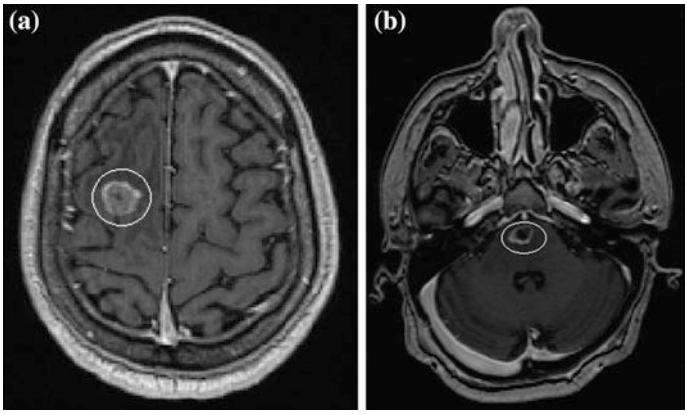

Fig. 2 Example of input MR axial slice with the bounding area (*white ellipsoid*), selected by the user, containing the tumor: **a** lesion without necrosis; **b** lesion with necrosis (*dark area*)

We used an ellipsoidal ROI selection tool, because it is widely provided by commercial medical imaging applications. This pseudocircular selected area is then enclosed and zero-padded into the minimum box in order to deal with a rectangular image during the following processing phases. The flow diagram of the overall segmentation method is shown in Fig. 3.

3.1 Pre-processing

Some pre-processing operations are applied on masked input images after the bounding region selection accomplished by the user, in order to improve segmentation results (Fig. 2a).

First of all, the range of intensity values of the selected part is expanded to extract the ROI more easily. Thereby, a contrast stretching operation is applied by means of a linear intensity transformation that converts the input intensity r values into the full dynamic range $s \in [0, 1]$.

A smoothing operation, using an average filter, is also required to remove the MRI acquisition noise (i.e. due to magnetic field non-uniformities). The application of the pre-processing steps on a cropped input image (Fig. 2a) is shown in Fig. 4b. The image contrast is visibly enhanced.

3.2 ROI Segmentation

Since the *FCM* algorithm classifies input data, the achieved clusters are represented by connected-regions and the corresponding boundaries are closed even when holes

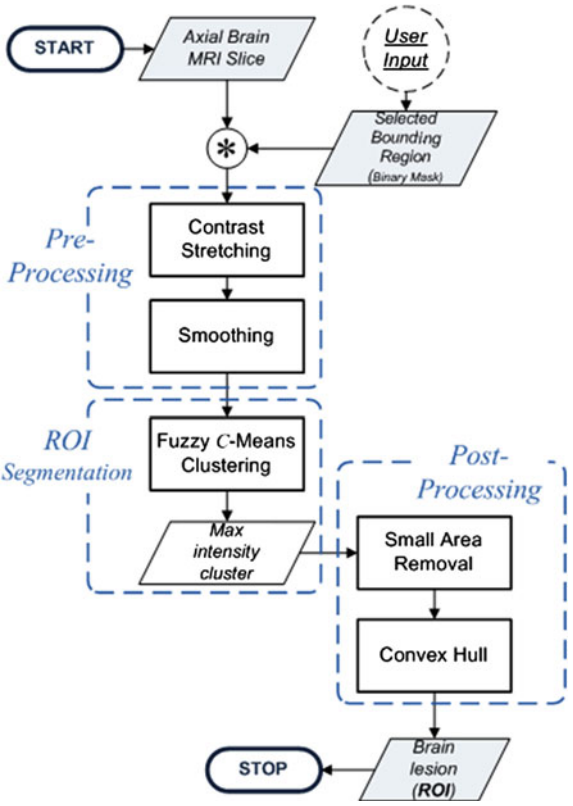

Fig. 3 Flow diagram of the proposed brain lesion segmentation method

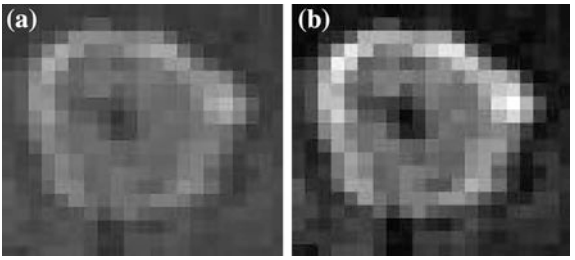

Fig. 4 Pre-Processing phase: **a** detail of the input MR image (part of the area inside the selected bounding region in Fig. 2a containing the tumor); **b** image after pre-processing steps

are present. This fact is very important in radiotherapy or radiosurgery treatment planning, because lesion segmentation is a critical step that must be performed accurately and effectively.

FCM cluster analysis is an iterative technique belonging to the realm of unsupervised machine learning [13, 14]. It classifies a dataset (i.e. a digital image) into groups (regions). Mathematically, the goal of this algorithm is to divide a set $X = \{\mathbf{x}_1, \mathbf{x}_2, \ldots, \mathbf{x}_N\}$ of N objects (statistical samples represented as vectors

belonging to n-dimensional Euclidean space $\mathfrak{R}^n$.) into C clusters (partitions of the input dataset) [15]. A partition P is defined as a set family $P = \{Y_1, Y_2, \ldots, Y_C\}$.

The crisp version (*K-Means*) states that the clusters must be a proper subset X ($\varnothing \subset Y_i \subset X, \forall i$) and their set union must reconstruct the whole dataset ($\bigcup_{i=1}^{C} Y_i = X$). Moreover, the various clusters are mutually exclusive ($Y_i \cap Y_j = \varnothing, \forall i \neq j$), i.e. each feature vector may belong to only one group. Whereas, a fuzzy partition P is defined as a fuzzy set family $P = \{Y_1, Y_2, \ldots, Y_C\}$ such that each object can have a partial membership to multiple clusters. The matrix $\mathbf{U} = [u_{ik}] \in \mathfrak{R}^{C \times N}$ defines a fuzzy C-partition of the set X through C membership functions $u_i : X \to [0, 1]$, whose values $u_{ik} := u_i(x_k) \in [0, 1]$ are interpreted as membership grades of each element $\mathbf{x}_k$ to the i-th fuzzy set (cluster)Y_i and have to satisfy the constraints in (1). Briefly, the sets of all the fuzzy C-partitions of the input X are defined by: $M_{fuzzy}^{(C)} = \left\{\mathbf{U} \in \mathfrak{R}^{C \times N} : u_{ik} \in [0, 1]\right\}$. From an algorithmic perspective, FCM is an optimization problem where an objective function must be iteratively minimized using the least-squares method. The fuzziness of the classification process is defined by the weighting exponent m.

$$\begin{cases} 0 \leq u_{ik} \leq 1 \\ \sum_{i=1}^{C} u_{ik} = 1, \quad \forall k \in [1, N] \\ 0 < \sum_{k=1}^{N} u_{ik} < N, \quad \forall i \in [1, C] \end{cases} \tag{1}$$

The *FCM* algorithm is applied just on pixels included in the selected ellipsoidal bounding region. Therefore, the zero-valued background pixels, added with zero-padding, are never considered. In particular, two clusters are employed ($C = 2$) in order to suitably classify a hyper-intense lesion from the healthy part of the brain. In fact, in contrast-enhanced MR brain scans, metastases have a brighter core than periphery and distinct borders distinguishing them from the surrounding normal brain tissue [16].

As the brain tumors are imaged as hyper-intense regions, during the defuzzification step, the pixels that have the maximum membership with the brightest cluster are selected. Figure 5a and 5b show two segmentation results achieved using the FCM clustering algorithm.

3.3 *Post-processing*

In some cases, central areas of the lesions could comprise necrotic tissue. For radiotherapeutic purposes, also these necrotic areas must be included in the target volume during the treatment planning phase.

A small area removal operation is used to delete any unwanted connected-components included in the highest intensity cluster. These small regions

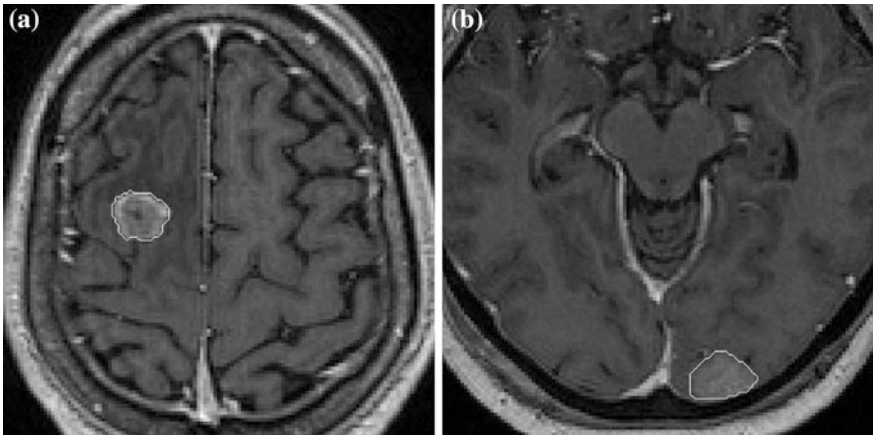

Fig. 5 Brain lesion segmentation using *FCM* clustering: **a** output of the MR image shown in Fig. 2a; **b** result obtained on another input MR image. (2× zoom factor)

may be due to anatomical ambiguities when the lesion is situated near high valued pixels (i.e. cranial bones or the corpus callosum).

Lastly, a *convex hull algorithm* [17] is performed to envelope the segmented lesion in the smallest convex polygon containing the automatically segmented ROI. In fact, brain lesions have a nearly spherical or pseudospherical appearance [16]; this also justifies the choice of an ellipsoidal ROI selection tool for the initial bounding region definition. Moreover, to include any necrosis inside the segmented ROI, this operation comprises hole filling too. An example is shown in Fig. 5b, where both the boundaries with and without the convex hull application are superimposed. Two examples are shown in Fig. 6a and 6b, where both the boundaries without and with the convex hull application are super-imposed.

4 First Experimental Results

To evaluate the accuracy of the proposed segmentation method, several measures were calculated by comparing the automatically segmented ROIs (achieved by the proposed approach) with the target volume manually contoured by a neurosurgeon (considered as our "gold standard"). Supervised evaluation is used to quantify the goodness of the segmentation outputs.

Area-based metrics and distance-based metrics are calculated for all slices of each MR image series, according to the definitions reported in Fenster & Chui [18] and Cárdenes et al. [19]. As evidenced in Figs. 5a and 5b, the proposed segmentation approach achieves correct results even with inhomogeneous input data.

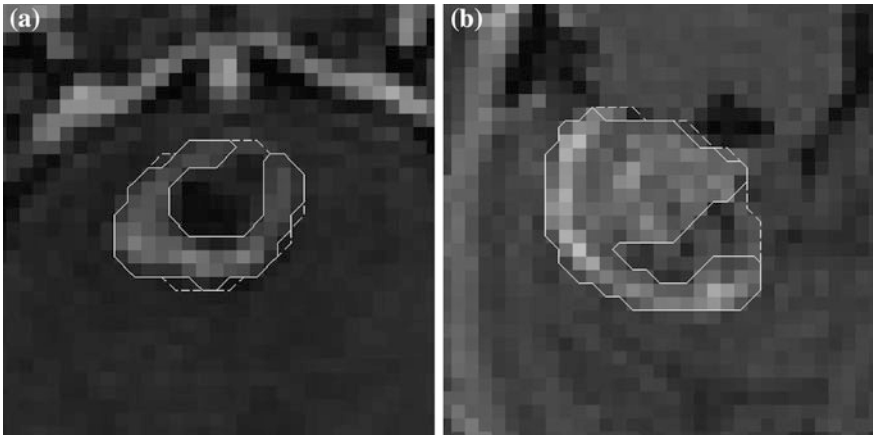

Fig. 6 Brain lesion segmentation without convex hull (*solid line*) and with convex hull application (*dashed line*): **a** output of the MR image shown in Fig. 2b; **b** a further example with necrotic tissue. (8× zoom factor)

4.1 Dataset Composition

The initial dataset is composed of 5 patients affected by brain tumors, who were treated with the Leksell Gamma Knife® stereotactic radio-surgical device. Each MRI series was acquired, just before treatment execution, to be used during the treatment planning phase.

MR images used in the segmentation trials were "T1w FFE" (T1weighted Fast Field Echo) sequences scanned with 1.5 Tesla MRI equipment (Philips Medical Systems, Eindhoven, the Netherlands). Brain lesions appear as hyper-intense zones with, in some cases, a dark area due to necrotic tissue.

4.2 Segmentation Evaluation Metrics

Area-based metrics quantify the similarity between the segmented regions through the proposed method (R_A) and our "gold standard" (R_T). Thus, the region containing "true positives" ($R_{TP} = R_A \cap R_T$) and "false negatives" ($R_{FN} = R_T - R_A$) are defined. In our experimental trials, we used the most important representative evaluation indices: Dice Similarity $DS = 2|R_{TP}| / (|R_A| + |R_T|) \times 100$, Jaccard index $JC = |R_A \cap R_T| / |R_A \cup R_T| \times 100$, Sensitivity aka True Positive Fraction $TPF = |R_{TP}| / |R_T| \times 100$, and Specificity aka False Negative Fraction $FNF = |R_{FN}| / |R_T| \times 100$.

In order to evaluate the contour discrepancy, the distance between the automatically generated boundaries (defined by the vertices $A = \{\mathbf{a}_i : i = 1, 2, \ldots, K\}$) and the manually traced boundaries ($T = \{\mathbf{t}_j : j = 1, 2, \ldots, N\}$) was also estimated.

Table 1 Values of area-based and distance-based metrics obtained on the segmented brain lesions for each patient

Dataset	$DS_{\%}$	$JC_{\%}$	$TPF_{\%}$	$FNF_{\%}$	*MAD*	*MAXD*	*H*
#1	96.29	93.00	96.70	1.87	0.193	0.955	1.471
#2	96.04	92.42	96.12	1.40	0.172	1.000	1.414
#3	94.77	90.15	95.15	2.37	0.290	1.069	1.833
#4	93.78	88.58	96.34	2.88	0.481	1.805	1.828
#5	94.61	89.94	94.97	2.40	0.376	1.472	1.637
AVG ± SD	95.10 ± 1.05	90.82 ± 1.84	95.86 ± 0.76	2.18 ± 0.57	0.302 ± 0.13	1.260 ± 0.37	1.636 ± 0.20

The following distances (expressed in pixels) were calculated: Mean Absolute Difference (*MAD*), Maximum Difference (*MAXD*), and Hausdorff distance (*H*).

In Table 1 the values of both area-based and distance-based metrics obtained in the experimental ROI segmentation tests are shown. High *DS* and *JC* ratios indicate excellent segmentation accuracy. In addition, the average value of *TPF* (sensitivity) proves that the proposed method correctly detects the "true" pathological areas. On the other hand, the very low *FNF* ratio (specificity) involves the ability of not detecting wrong parts within the automatically segmented ROI. Moreover, achieved distance-based indices are coherent with area-based metrics. These findings show the great reliability of the proposed approach even when MR images are affected by acquisition noise and artifacts. Good performance is guaranteed also with poor contrast images or lesions characterized by irregular shapes.

5 Conclusions and Future Works

In this paper an original application of the *FCM* clustering algorithm was presented. The unsupervised learning technique was used to support brain tumor segmentation for Gamma Knife treatments. The proposed semi-automatic segmentation approach was tested on a dataset made up of 5 MRI series, calculating both area-based and distance-based metrics. The achieved experimental results are very encouraging and they show the effectiveness of the proposed approach.

However, it is not always possible to identify the actual tumor extent using the only MRI modality. The combination of multimodal imaging might address this important issue [2]. Surgery, chemotherapy and radiation therapy may alter the acquired MRI data concerning the tumor bed. Therefore, further studies are planned to use a multimodal approach to the target volume selection, which integrates MRI with MET-PET (Methionine—Positron Emission Tomography) imaging [20]. In this way, MR images will highlight the morphology of the lesion volume (Gross Tumor Volume, *GTV*), while PET images will provide information on metabolically active areas (Biological Target Volume, *BTV*) [21].

The proposed approach for lesion segmentation from brain MRI, properly integrated with PET segmentation, would provide a comprehensive support for the precise identification of the region to be treated (Clinical Target Volume, *CTV*) during Gamma Knife treatment planning. The *CTV* will thus be outlined by the physician, through registration and fusion of segmented volumes on PET/MR images.

Acknowledgments This work was supported by "Smart Health 2.0" MIUR project (PON 04a2_C), approved by MIUR D.D. 626/Ric and 703/Ric.

References

1. Beavis, A.W., Gibbs, P., Dealey, R.A., Whitton, V.J.: Radiotherapy treatment planning of brain tumours using MRI alone. British J. Radiol. **71**(845), 544–548 (1998). doi:10.1259/bjr.71.845.9691900
2. Joe, B.N., Fukui, M.B., Meltzer, C.C., Huang, Q.S., Day, R.S., Greer, P.J., Bozik, M.E.: Brain tumor volume measurement: comparison of manual and semiautomated methods. Radiology **212**(3), 811–816 (1999). doi:10.1148/radiology.212.3.r99se22811
3. Leksell, L.: Stereotact. Radiosurgery. J. Neurol. Neurosurg. Psychiatry **46**, 797–803 (1983). doi:10.1136/jnnp.46.9.797
4. Luxton, G., Petrovich, Z., Jozsef, G., Nedzi, L.A., Apuzzo, M.L.: Stereotactic radiosurgery: principles and comparison of treatment methods. Neurosurgery **32**(2), 241–259 (1993). doi:10.1227/00006123-199302000-00014
5. Militello, C., Rundo, L., Gilardi, M.C.: Applications of imaging processing to MRgFUS treatment for fibroids: a review. Transl. Cancer Res. **3**(5), 472–482 (2014). doi:10.3978/j.issn.2218-676X.2014.09.06
6. Salerno, S., Gagliardo, C., Vitabile, S., Militello, C., La Tona, G., Giuffrè, M., Lo Casto, A., Midiri, M.: Semi-automatic volumetric segmentation of the upper airways in patients with pierre robin sequence. Neuroradiol. J. (NRJ) **27**(4), 487–494 (2014). doi:10.15274/NRJ-2014-10067
7. Militello, C., Vitabile, S., Russo, G., Candiano, G., Gagliardo, C., Midiri, M., Gilardi, M.C.: A semi-automatic multi-seed region-growing approach for uterine fibroids segmentation in MRgFUS treatment. In: 7th International Conference on Complex, Intelligent, and Software Intensive Systems, CISIS 2013, art. no. 6603885, pp. 176–182
8. Aslian, H., Sadeghi, M., Mahdavi, S.R., Babapour Mofrad, F., Astarakee, M., Khaledi, N., Fadavi, P.: Magnetic resonance imaging-based target volume delineation in radiation therapy treatment planning for brain tumors using localized region-based active contour. Int. J. Radiat. Oncol. Biol. Phys. **87**(1), 195–201 (2013). doi:10.1016/j.ijrobp.2013.04.049. ISSN: 0360-3016
9. Xie, K., Yang, J., Zhang, Z.G., Zhu, Y.M.: Semi-automated brain tumor and edema segmentation using MRI. Eur. J. Radiol. **56**(1), 12–19. (2005). doi:10.1016/j.ejrad.2005.03.028. ISSN: 0720-048X
10. Mazzara, G.P., Velthuizen, R.P., Pearlman, J.L., Greenberg, H.M., Wagner, H.: Brain tumor target volume determination for radiation treatment planning through automated MRI segmentation. Int. J. Radiat. Oncol. Biol. Phys. **59**(1), 300–312 (2004). doi:10.1016/j.ijrobp.2004.01.026. ISSN: 0360-3016
11. Bauer, S., Nolte, L.P., Reyes, M.: Fully automatic segmentation of brain tumor images using support vector machine classification in combination with hierarchical conditional random field regularization. In: Medical Image Computing and Computer-Assisted Intervention—MICCAI 2011. Lecture Notes in Computer Science, vol. 6893, pp. 354–361 (2011). doi:10.1007/978-3-642-23626-6_44
12. Hall, L.O., Bensaid, A.M., Clarke, L.P., Velthuizen, R.P., Silbiger, M.S., Bezdek, J.C.: A comparison of neural network and fuzzy clustering techniques in segmenting magnetic resonance images of the brain. IEEE Trans. Neural Netw. **3**(5), 672–682 (1992). doi:10.1109/72.159057
13. Militello, C., Vitabile, S., Rundo, L., Russo, G., Midiri, M., Gilardi, M.C.: A fully automatic 2D segmentation method for uterine fibroid in MRgFUS treatment evaluation. Computers in Biology and Medicine, **62**, 277–292 (2015). doi:10.1016/j.compbiomed.2015.04.030
14. Chuang, K.S., Tzeng, H.L., Chen, S., Wu, J., Chen, T.J.: Fuzzy c-means clustering with spatial information for image segmentation. Comput. Med. Imaging Graph. **30**(1), 9–15 (2006). doi:10.1016/j.compmedimag.2005.10.001. ISSN: 0895-6111
15. Pal, N.R., Bezdek, J.C.: On cluster validity for the fuzzy c-means model. IEEE Trans. Fuzzy Syst. **3**(3), 370–379 (1995). doi:10.1109/91.413225

16. Ambrosini, R.D., Wang, P., O'Dell, W.G.: Computer-aided detection of metastatic brain tumors using automated three-dimensional template matching. J. Magn. Reson. Imaging **31**(1), 85–93 (2010). doi:10.1002/jmri.22009
17. Zimmer, Y., Tepper, R., Akselrod, S.: An improved method to compute the convex hull of a shape in a binary image. Pattern Recogn. **30**(3), 397–402 (1997) doi:10.1016/S0031-3203(96)00085-4. ISSN: 0031-3203
18. Fenster, A., Chiu, B.: Evaluation of segmentation algorithms for medical imaging. In: 27th Annual International Conference of the Engineering in Medicine and Biology Society, IEEE-EMBS 2005, pp. 7186–7189 (2005). doi:10.1109/IEMBS.2005.1616166
19. Cárdenes, R., de Luis-García, R., Bach-Cuadra, M: A multidimensional segmentation evaluation for medical image data. Comput. Methods Prog. Biomed. **96**(2), 108–124 (2009). doi:10.1016/j.cmpb.2009.04.009. ISSN: 0169-2607
20. Levivier, M., Wikler Jr., D., Massager, N., David, P., Devriendt, D., Lorenzoni, J., et al.: The integration of metabolic imaging in stereotactic procedures including radiosurgery: a review. J. Neurosurg. **97**, 542–550 (2002). doi:10.3171/jns.2002.97.supplement5.0542
21. Stefano, A., Vitabile, S., Russo, G., Ippolito, M., Sardina, D., Sabini, M.G., et al. A graph-based method for PET image segmentation in radiotherapy planning: a pilot study. In: Petrosino, A. (ed.) Image Analysis and Processing, vol. 8157, pp. 711–720. Springer, Berlin (2013). doi:10.1007/978-3-642-41184-7_72

http://www.springer.com/978-3-319-33746-3

Advances in Neural Networks
Computational Intelligence for ICT
Bassis, S.; Esposito, A.; Morabito, F.C.; Pasero, E. (Eds.)
2016, XVI, 539 p. 158 illus., 132 illus. in color.,
Hardcover
ISBN: 978-3-319-33746-3